CLRC

Spares

Technical Report
RAL-TR-96-060

Global Evaluation of Sea-Surface Temperature Retrievals from the Along-Track Scanning Radiometer Through Comparison with the NOAA Operational Analysis

M J Murray M R Allen and C T Mutlow

August 1996

COUNCIL FOR THE CENTRAL LABORATORY OF THE RESEARCH COUNCILS

Enquiries about copyright, reproduction and requests for
additional copies of this report should be addressed to:

The Central Laboratory of the Research Councils
Library and Information Services
Rutherford Appleton Laboratory
Chilton
Didcot
Oxfordshire
OX11 0QX
Tel: 01235 445384   Fax: 01235 446403
E-mail library@rl.ac.uk

ISSN 1358-6254

Global evaluation of sea-surface temperature retrievals from the Along-Track Scanning Radiometer through comparison with the NOAA Operational Analysis

M. J. Murray, M. R. Allen and C. T. Mutlow
Space Science Department, Rutherford Appleton Laboratory
Chilton, Didcot, OX11 0QX, UK
e-mail: m.r.allen@rl.ac.uk

ERS-RL-TN-2175/96 — July, 1996

Abstract

The Along-Track Scanning Radiometer (ATSR) has provided almost five years of global sea-surface temperature (SST) observations since its launch on ESA's ERS-1 satellite in July 1991. Comparison of these data with the NOAA Operational Analysis, based on *in situ* measurements and Advanced Very High Resolution Radiometer (AVHRR) data, confirms that the three-channel dual-angle-view ATSR SST retrieval scheme achieved its design objective of accurate and independent SST observations even in the presence of severe atmospheric aerosol contamination due to the eruption of Mount Pinatubo. Clear scope for improvement remains, however, in the initial ATSR two-channel and single-view SST retrievals.

1 Introduction

Sea-surface temperature (SST) is a key parameter determining the behaviour of the ocean-atmosphere interface. A consistent, continuous and global SST field with an absolute accuracy of around 0.3K has been called for to satisfy the requirements of ocean and climate research (e.g. Harries *et al.*, 1983; Allen *et al.*, 1994). Conventional observations made from ships and buoys are concentrated in shipping lanes and sparse in the Southern hemisphere. Observations made by satellite-borne infrared radiometers provide near-global coverage, but SST retrieval is inevitably compromised by the difficulty of adequately compensating for atmospheric effects, such as clouds, water vapour and aerosols.

Over 15 years of SST measurements have been made by the Advanced Very High Resolution Radiometer (AVHRR) series of instruments on the NOAA TIROS-N series of operational satellites. These have provided global SSTs with a nominal accuracy of approximately 0.7K (Mc Clain *et al.*, 1985), and considerable effort has been devoted to the production of a consistent AVHRR SST record through the NASA Pathfinder project. In general, efforts at improving AVHRR SST retrievals have involved using data from other sources, such as quality-controlled *in situ* buoy observations, to devise empirical algorithms to convert AVHRR brightness temperatures into SST. This leads to a more accurate SST retrieval, at the cost of loss of independence of the various data sources.

AVHRR SST retrievals were found to be severely compromised by atmospheric aerosol contamination such as occurred after the eruption of Mount Pinatubo in June 1991. By September 1991 the number of day-time SST retrievals dropped close to zero in the tropics, as the cloud-clearing algorithms were found to be unreliable in these conditions; negative biases greater than 1K have been reported in those SST retrievals which were achieved (Reynolds, 1993). A variety of aerosol correction algorithms have since been proposed.

The first Along-Track Scanning Radiometer (ATSR-1) is a four-channel, dual-view, self-calibrating, infrared radiometer with spatially co-registered spectral channels centred at 1.6μm, 3.7μm, 10.8μm and 12.0μm. The 1.6μm channel is useful only in day-time and its primary purpose is cloud identification. The key experimental feature of ATSR is that it views the same point on the ocean surface twice, over an interval of approximately 100 seconds, at two different angles through the atmosphere as the satellite passes overhead. This allows a "dual-view" retrieval in which two different atmospheric path lengths are utilized to quantify and correct for the effects of atmospheric emissions and absorption. ATSR was designed to measure SSTs to an accuracy of 0.3K without recourse to surface observations. A standard set of climatological radiosonde profiles was used in the generation of the coefficients in the retrieval algorithm (Závody *et al.*, 1994) but no post-launch corrections have been applied to bring the ATSR data into agreement with other SST observations: hence it represents a completely independent dataset. Other features of the ATSR design include the on-board calibration, and the use of actively cooled detectors (see Delderfield *et al.*, 1986, Edwards *et al.*, 1990).

The absolute accuracy of ATSR SSTs can only be evaluated through validation against accurately collocated *in situ* observations of ocean skin temperature (Minnett, 1991). Considerable effort has been made in this direction (see, for example: Mutlow *et al.*, 1994; Barton *et al.*, 1995; Forrester and Challenor, 1995; Donlon and Robinson, 1996). Nevertheless the practical difficulty of making accurate *in situ* measurements of skin SST means that the size of validation datasets remains limited. An alternative approach, previously adopted by Harrison and Jones (1993), is to compare the ATSR data with an independent SST analysis. This cannot provide an absolute measure of instrument accuracy, since collocation noise would typically dominate individual ATSR-analysis differences, but it enables the examination of large-scale patterns of bias to search for the spatio-temporal signature of atmospheric contamination. We focus on a comparison with the NOAA operational SST analysis, also popularly known as "Reynold's analysis", widely regarded as the best available SST analysis on this resolution.

2 NOAA Operational Analysis

The NOAA operational SST analysis (Reynolds, 1988; Reynolds and Marisco, 1993; Reynolds and Smith, 1994), hereafter NOAA-OA, uses a blend of *in situ* (ship and buoy) and AVHRR data, to produce global weekly-mean SSTs on a one-degree grid. These data are compiled using a two-step procedure in which satellite data are initially corrected for any (spatio-temporally varying) bias by using them to provide second derivative information in a solution of Poisson's equation anchored to *in situ* data. An optimal interpolation (OI) scheme is then used to produce a continuous analysis. Thus the absolute values of buoy and ship data are given a relatively high weight, and only the derivatives of the satellite are, in effect, used in the OI. *In situ* SSTs outside the range $-2°C < T < 35°C$ are discarded, as are those data for which the SST anomaly lies outside ± 3.5 times the climatological standard deviation. The contributing SSTs represent a mixture of day-time and night-time observations.

3 ATSR data

A variety of products are derived from ATSR data (Bailey, 1993) but this analysis is based on the spatially-Averaged Sea-Surface Temperature (ASST) product. These data comprise half-degree, spatially-averaged SSTs with associated temporal, positional and confidence information. The data considered here were acquired during the four-year period August 1991 – July 1995 inclusive. These data have been made available on a CD-ROM set (Murray, 1995) available from the ATSR Science Team at RAL.

The ATSR SST retrieval scheme follows that of McClain *et al.* (1985), where SST is given by a linear combination of infrared brightness temperatures:

$$\mathrm{SST} = a_0 + \sum_{i=1}^{N} a_i T_i$$

where the a_i are constant (latitude-dependent) coefficients and T_i is the cloud-free scene brightness temperature as observed by ATSR either in the nadir or forward view. A range of retrieval algorithms are possible with this geometry; in the most accurate, a dual-view three-spectral-channel (3.7, 10.8 and 12.0μm) retrieval which can be used only at night, i ranges from 1 to 6. Dual-view, two-channel (10.8 and 12.0μm) retrievals are used for day-time observations when sunglint contaminates the 3.7μm brightness temperatures, and also for all retrievals after the premature loss of the 3.7μm channel on 27th May, 1992. Single-view (nadir only) SSTs are computed for comparison with the dual-view product, and also to provide an estimate of SST where cloud cover or operational constraints make it impossible to obtain a spatially co-registered dual-view retrieval. Separate coefficients are derived for each retrieval scheme using global radiosonde sets and an atmospheric radiative transfer model; three characteristic atmospheric profiles are used (polar, mid-latitude or tropical) and latitude-dependent coefficients are obtained by linear interpolation between them. A complete description of the ATSR SST retrieval is given in Závody *et al.*(1994, 1995).

ATSR data were averaged into a one-degree, weekly spatio-temporal grid matching the spatial and temporal division of the NOAA-OA. Only data within 6K of the Global Ocean Surface Temperature Atlas (GOSTA – Bottomley *et al.*, 1990) climatology were used; this requirement excluded less than 0.3% of day-time and approximately 4% of night-time ATSR data. Rejection was overwhelmingly because the ATSR SSTs were too cold, probably due to cloud contamination. A more conservative climatological check would improve the ATSR/NOAA-OA agreement and might also help in the identification of more subtle sources of bias, but would also introduce the risk of excluding valid data in regions of high interannual SST variability. Likewise, a consistency check between day-time and night-time ATSR data, as used in Jones *et al.* (1996), would also reduce bias and noise. This is to be investigated in subsequent work.

In the case of night-time data, most of the cold SSTs were observed in the Southern Ocean at latitudes south of 30°S, although a significant contribution from northern latitudes occurs in the summer months in that hemisphere. Too-cold day-time observations usually arise at mid-latitudes in the Northern hemisphere during the summer months. Unsurprisingly the cold bias associated with inadequate cloud-clearing is much less than with night-time SSTs, since the availability of the 1.6μm reflectances enables much better cloud identification in daylight.

ATSR day-time and night-time observations have been considered separately throughout this paper, as have dual-view and single-view (that is, nadir only) observations.

4 Comparison of ATSR and NOAA-OA SSTs

Any satellite-based SST measurement represents the temperature of a water layer less than 0.1 mm thick; this is typically several tenths of a degree cooler than the temperature a few millimeters below it, which in turn may be either cooler or warmer than the "bulk" temperature at 1m depth, depending on the state of the near-surface thermocline. See Schluessel *et al.* (1990) for a discussion of the factors influencing the sense and magnitude of this "skin/bulk" temperature difference. In general, skin temperature is subject to much stronger diurnal variation than the bulk temperature as defined above, with a peak skin SST occurring in the late afternoon as a result of solar heating, at which time the ocean skin may be warmer than the bulk temperature. However, most ATSR day-time observations are made between 10:30 and 11:00 local time, and night-time observations about twelve hours later. At these times it is likely that, on average, the ocean skin will be cooler than the bulk temperature. As NOAA-OA uses absolute temperatures from *in situ* SSTs, and only the derivatives of the satellite SSTs, it is representative of ocean bulk temperature.

This comparison uses NOAA-OA SSTs warmer than $-1.8°$, the value used as an ice mask, and excludes data flagged as land or ice in the GOSTA climatology. Improved ice identification is an area of priority activity identified by this survey.

4.1 Zonal mean differences

Initially we investigate time-latitude plots of zonally-averaged, weekly-mean, one-degree SST fields. The choice of zonal mean fields is made as the major sources of bias between ATSR and NOAA-OA (*i.e.* aerosols, cloud contamination and the skin-bulk effect) should, to a first approximation, appear zonally symmetric. Only ocean data have been included (no lakes or inland seas). All temperatures are given in Kelvin, and shown in the range 268K to 304K for absolute SSTs, and -2.0K to $+0.5$K for ATSR–NOAA-OA differences; therefore a negative difference indicates an ATSR SST is colder than that from NOAA-OA. As explained above, ATSR SSTs might be expected to be slightly cooler than NOAA-OA due to the skin-bulk effect, and may be further affected by inadequate compensation for atmospheric contamination. Except where specified otherwise, the figures cover the four-year period, August 1991 – July 1995 inclusive.

Figure 1 represents the global SST field from NOAA-OA, and Figure 2 shows the equivalent field for night-time, dual-view ATSR data. As described above, where possible, night-time SST retrievals utilize the 11, 12 and 3.7μm data. However no 3.7μm data were transmitted to ground during the period 6th August–13 September 1991, and the 3.7μm channel was permanently lost on 27th May 1992. Subsequent to the loss of the 3.7μm data, night-time SST retrievals were initially about 0.6K cooler than the previous three-channel retrievals. Complications arising from the failure, resulted in a short period of missing data around this time (evident as black horizontal lines).

Figure 3 shows the difference between the ATSR dual-view night-time SSTs and NOAA-OA. Aerosol contamination due to the Mount Pinatubo plume is apparent both at the start of the mission, and subsequent to the failure of the 3.7μm channel in May 1992. However near complete elimination of the Pinatubo aerosol is achieved when ATSR 3.7μm data are available.

This comparison highlights a parabolic anomaly in the Southern hemisphere during October 1991 – March 1992. This feature is apparent in the NOAA-OA, with affected SSTs being subject to a negative bias of up to 2K in this region (Reynolds, 1992). This is due to an AVHRR calibration anomaly affecting the 3.7μm data and thus the night-time SSTs. The problem occurs at certain solar/satellite geometries when the satellite moves out of earth's shadow. The effect was exacerbated by the aerosol-corrected algorithm in use at the time, by the shortage of day-time SSTs, and the usual lack of *in situ* data in the region.

Comparison of ATSR data with and without 3.7μm data suggests the standard deviation of the ATSR–NOAA-OA differences rose from 0.7K to 0.9K post-3.7μm failure. These figures are based on comparing 40 weeks of data immediately before 27th May 1992 with 40 weeks of data shortly afterwards. Only SSTs north of 10°S were considered in both datasets, to exclude the effects of the anomaly in the NOAA-OA. These figures give some indication of the impact of the loss of the 3.7μm channel, but are not an indication of the absolute accuracy of either dataset since the ATSR and NOAA-OA data have not been accurately collocated; that is, we are comparing weekly $1° \times 1°$ areas with no guarantee that observations in the two datasets have been taken at the same time in that spatio-temporal region. Moreover, the smoothing of the NOAA-OA would result in a non-zero standard deviation in the difference between the two datasets, even if the unsmoothed data were in perfect agreement.

The success of the ATSR SST 3-channel, dual-view retrieval in conditions of severe aerosol contamination is clearly apparent, and the value of the dual-view observations can be established by comparing this result with the equivalent comparison using ATSR nadir-only SSTs, as shown in figure 4.

Figure 4 shows the ATSR–NOAA-OA difference field using only ATSR night-time nadir-view information the SST retrieval. It is clear that the availability of the 3.7μm data enables a much improved SST retrieval in the presence of aerosols. However, unlike the dual-view retrieval, aerosol-induced biases of up to 1.5K are present in the nadir-only SSTs, as indicated by the equator-to-pole gradients in the difference field.

The difference fields shown in Figures 3 and 4 both exhibit a seasonal cycle in equatorial regions and at mid-latitudes in the Northern hemisphere. This cycle appears more marked in the case of the nadir-only SSTs, and is least evident in the case of the dual-view SSTs to which the 3.7μm data contributed. Since we would expect some seasonality in atmospheric contamination from both aerosol and water vapour, this result is not surprising. Further examination of this seasonal cycle in these biases might prove a useful approach to understanding their origins.

Figures 5 and 6 show the (ATSR−NOAA-OA) difference fields using ATSR day-time dual-view, and day-time nadir-view respectively. ATSR day-time SST retrievals use only the 11 and 12μm brightness temperatures, with the 1.6μm data used for cloud clearing. This two-channel retrieval does not deal with aerosol contamination as effectively as the three-channel night-time retrieval. Nevertheless the improvement of the dual-view with respect to the nadir-only SST retrieval is again demonstrated.

Both the latter two figures exhibit noisiness at high latitudes in the Northern hemisphere. The low sea/land ratio in this region may be partially responsible for this, as may an inadequate ice mask. Another contributory factor is that, in this initial processing phase, ATSR dual-view SSTs could not be processed over a 200km wide strip of the Northern Atlantic as shown in Figure 16. This is simply because orbits were initially processed individually, making it impossible to compute a dual-view SST if the necessary data was acquired across the (arbitrary) junction between one orbit and the next. It should be straightforward to rectify this in subsequent reprocessing. A strong seasonal cycle at mid-latitudes in the Northern hemisphere is again apparent, and appears particularly clearly in the dual-view SST comparison.

4.2 Time series from selected regions

To allow more quantitative comparison than is possible in Hofmoller diagrams, we show time series of weekly-mean temperature differences over selected latitude ranges. High-latitude data have been omitted from the comparisons to avoid the effects of ice contamination, and only gridboxes where both datasets have valid SSTs are used in compiling regional mean differences, to minimize sampling noise.

Figure 7 shows the difference between ATSR dual-view SSTs and the NOAA-OA in the latitude range 70°S–70°N, with ATSR day-time and night-time SSTs shown separately. During the period when the 3.7μm data were available, ATSR night-time SSTs exhibit a cold bias of only 0.3K with respect to the NOAA-OA. Subsequent to the May 1992 failure, a sudden drop of around 0.7K occurs, after which night-time SSTs follow a similar trend to day-time SSTs, but are consistently cooler than the latter by about 0.2K.

Considering the day-time difference, the ATSR SSTs are approximately 0.8K cooler than the NOAA-OA SSTs in 1991. This is larger than expected due to the skin-bulk difference, and the temporal evolution of the bias suggests that it can be attributed primarily to inadequate compensation for atmospheric aerosols from Mount Pinatubo in the ATSR day-time retrieval. In 1992 and the first half of 1993, the difference slowly reduces as the Pinatubo aerosols dissipate, until it stabilizes at a mean (ATSR−NOAA-OA) value of approximately −0.5K until October 1994 when a drop of around 0.2K is observed in the ATSR SSTs, discussed below.

The same comparison for tropical regions (30°S–30°N) is shown in Figure 8. Once again, the ATSR day-time SSTs become warmer with respect to the NOAA-OA as the Pinatubo aerosols reduce. As this is the region most affected by the aerosols, the trend is stronger than in the wider latitude band considered in the previous figure. For the ATSR day-time SSTs, the cold bias with respect to NOAA-OA reduces from around −1.2K in September 1991, to −0.4K in October 1993. However a relative downward trend in ATSR SSTs is apparent from the start of 1994. The exact origin of this trend remains to be firmly identified, but some contribution may be associated with the temperature of the ATSR detectors.

During 1994 and 1995, it became increasingly difficult for ATSR's on-board cooler to maintain the detector temperatures at their post-launch mean value of around 95K. To maximize the life of the cooler, temperatures were allowed to rise slightly, reaching 110K in 1996. This warming has most impact on the response of the 12μm detector and by 1995 may have begun to affect retrieved SSTs, particularly in humid tropical conditions (Závody, 1996, private communication). We stress that, through the unique on-board calibration of ATSR, we have the necessary information to model and correct for any long-term trend due to changes in detector temperature, so this should not ultimately compromise the temporal integrity of the dataset. The same trend is apparent in the difference timeseries for the ATSR night-time SSTs, although the dominant signal here is again the sudden cooling following 3.7μm failure in May 1992.

The value of the dual-view retrieval is apparent when we consider the corresponding time series using nadir-only ATSR SST retrievals. As shown in Figure 9, during the time of heaviest aerosol contamination in the tropics, nadir-only SSTs are cooler than the corresponding dual-view SSTs by up to 0.7K.

The drop in ATSR night-time SSTs subsequent to the failure of the 3.7μm channel is clearly a matter of concern. The loss of these data affected night-time retrievals in two ways: a two-channel SST retrieval algorithm using only 11 and 12μm data was necessarily adopted, and the cloud-identification tests which used 3.7μm data were lost. To estimate the relative importance of these two effects we attempt to quantify the reduced effectiveness of the cloud clearing by comparing all ASST night-time SSTs with those from relatively cloud-free regions. Each ATSR ASST value refers to a half-degree area which is divided into nine *cells*. Each cell is evaluated for cloudiness independently and, as a first approximation, we can presume that ASSTs in which eight or nine cells are registered as cloud-free are in fact not affected by any residual cloud contamination. This is clearly only a preliminary check – improved *post hoc* cloud correction schemes are to be implemented in a subsequent study (Jones *et al.*, 1996). Figure 10 shows a comparison of weekly-mean dual-view night-time SSTs in the latitude range 70°S–70°N; one average is computed using all SSTs, as in figure 7, and the other uses only those SSTs which arose from these "cloud free" areas. During the period when 3.7μm data were available, the weekly-mean temperature based on all SSTs remains very close to that derived only from 'clear' half-degree fields. After the 3.7μm data were lost, the weekly-mean based on cloud-free cells are warmer than the mean of all the SSTs, but by a factor of less than 0.1K. Although selection effects may compromise this comparison, it seems likely that most of the drop in ATSR night-time SSTs can be attributed to a bias between the three-channel and two-channel SST retrieval algorithms. This is encouraging, since eliminating this bias in the two-channel retrieval may simply require revised coefficients: this is clearly an urgent priority in the reprocessing programme.

As these comparisons are dominated by the effects of aerosols in equatorial regions, we now consider the mid-latitudes in both hemispheres. Figures 11 and 12 show the weekly-mean ATSR–NOAA-OA differences for the latitude bands 70°S–30°Sand 30°N–70°N respectively. As shown in Figure 11, ATSR SSTs average about 0.7K cooler than NOAA-OA values in mid-latitudes in the Southern hemisphere, with no clear aerosol-related trend. However there is a weak seasonal cycle in the bias, particularly in case of the ATSR day-time SSTs in the first two years of the mission, which appear warmest with respect to NOAA-OA in the Southern summer.

Figure 12 shows the corresponding plot for Northern mid-latitudes. A strong seasonal cycle is evident, with ATSR day-time SSTs peaking in the middle of Northern summers at temperatures in excess of NOAA-OA, but showing a cold bias of about 1.0K with respect to the latter in the winter. Night-time SSTs evaluated when 3.7μm data were available are approximately 0.4K cooler than NOAA-OA, with no sign of seasonal variation. Post May 1992, these SSTs show a weak seasonal cycle, with a cold bias ranging from about 0.9K in winter to 0.5K in summer compared to NOAA-OA. This points towards the need for seasonally-dependent two-channel retrieval algorithms, discussed further in the conclusions.

4.3 Geographic location of ATSR–NOAA-OA bias

As a preliminary investigation of the geographic location of the differences in the ATSR and NOAA-OA, we now consider global maps of time-averaged SST difference fields. Only ATSR dual-view data have been used. All temperatures differences are given in Kelvin, and shown in the range −2.0K to +0.5K.

Figure 13 shows a four-year average of ATSR–NOAA-OA using ATSR day-time dual-view SSTs. The missing band of data from Greenland through the North Atlantic and into the Mediterranean arises because the ATSR data downlink occurs in this area, as discussed above.

In general the ATSR SSTs show a cold bias of about 0.4K with respect to NOAA-OA. However, considerable geographic variation is evident. ATSR SSTs are around 1.0K cooler than those from NOAA-OA in the tropical West Pacific, possibly as a result of inadequate compensation for atmospheric water vapour. Saharan dust is likely to be responsible for a similar cold bias in ATSR SSTs evident around Africa's Ivory Coast.

Extensive regions in the N.W. Atlantic and N.W. Pacific exhibit ATSR SSTs up to 2K cooler than NOAA-OA SSTs; this may be associated with residual cloud contamination of ATSR data or a systematic dependence of the ATSR retrieval on local meteorological conditions (given that these features correspond to the Northern Hemisphere storm tracks). It might also be evidence of tropospheric aerosol contamination from the industrialised regions of North America and East Asia. Alternatively, given the close correspondence of the pattern to surface heat flux climatology, we may be seeing evidence of the skin-bulk effect. This clearly represents a promising avenue for further investigation.

ATSR SSTs are much warmer than the corresponding NOAA-OA SSTs in the Arctic and Hudson Bay regions. This is likely to be due to inconsistencies in ice flagging between the two datasets.

An intriguing aspect of the figure is the undulations in ATSR–NOAA-OA bias apparent off the U.S. Eastern seaboard. Since this is a region of strong SST gradients, we may be observing an artefact of the optimal interpolation used in the NOAA-OA, but the exact origins of this feature remain to be investigated. Similar structure is apparent in other regions where the SST is affected by western boundary currents, for example the Argentine and Japanese coasts.

Figure 14 shows the corresponding figure for those nine months of ATSR night-time SSTs for which the 3.7μm data were available. This is considerably noisier than the day-time figure (due to a much shorter integration time) and the ERS-1 3-day orbit repeat cycle (which dominated this period) is clearly visible. Nevertheless the pattern associated with water vapour which is so clear in the day-time data is absent, indicating the success of three-channel dual-view retrieval.

4.4 Dual–Nadir differences within ATSR data

In general, differences between the dual-view and nadir-only SST retrievals are attributable to absorption by atmospheric constituents which were not included in the calculation of the retrieval coefficients. The dual–nadir difference can thus be used as a tracer for atmospheric aerosols (recalling that the ATSR retrieval coefficients are based on an assumption of climatological background aerosol loading) and to a lesser extent may be affected by changes in total column water vapour. Figure 15 shows the zonally-averaged ATSR dual–nadir difference for night-time data. Prior to the failure of the 3.7μm channel and ignoring the first three weeks of operation when 3.7μm data were not available, the effects of the Mount Pinatubo aerosol plume are clear, with dual-view SSTs more than 1K warmer than the corresponding nadir-only values in the tropics. The heaviest aerosol load appears to be within 20° of the equator until November 1991. Until this time, the Southern hemisphere appears more heavily contaminated than the Northern hemisphere. However in the first months of 1992 there appears to be stronger transport into the Northern hemisphere. By May 1992, the aerosol load appears fairly evenly distributed over all latitude ranges.

Figure 16 shows the corresponding plot for day-time data. The aerosol plume appears well-confined within 30° from the equator until March 1992, after which time there appears to be a rapid movement into the Northern hemisphere. This in broad agreement with the observations of Baran and Foot (1994).

The close correspondence between the patterns of dual–nadir differences and the patterns of ATSR–NOAA-OA differences in the day-time and post-3.7-μm-failure night-time two-channel retrievals (figures 3 and 5) is encouraging, since it implies that the necessary information to correct these two-channel retrievals is indeed present in the ATSR data.

5 Conclusions

The most important result to emerge from this comparison is the success of the ATSR night-time dual-view SST retrievals using 3.7, 11 and 12μm data during a period of heavy atmospheric aerosol contamination. This result is particularly significant in that the coefficients in the retrieval algorithm were determined before launch, and assume only climatological background levels of aerosol: the implication is that a three-channel, dual-view SST retrieval is genuinely insensitive to significant changes in atmospheric composition, as anticipated in the design of this mission.

During the time when these data were all available, ATSR night-time SSTs are around 0.3K cooler than NOAA-OA, an amount which is consistent with the skin/bulk temperature difference and the slightly cooler temperatures expected at night-time relative to the NOAA-OA diurnal average. The value of the dual-view retrieval is confirmed by the comparison with the nadir-only retrieval in which a cold bias of up to 2K can be attributed to the effect of aerosols, and in which the location of the Pinatubo plume can be clearly seen.

As discussed above, the loss of the 3.7μm channel in May 1992 affected night-time retrievals in two ways; a two-channel SST retrieval algorithm using only 11 and 12μm data was necessarily adopted, and the cloud-identification tests which used 3.7μm data were lost. The two-channel algorithm appears to be subject to a systematic cold bias, and is compromised by the presence of atmospheric aerosols. An improved algorithm which incorporates a correction for the Pinatubo aerosols is under development.

Inadequate cloud-clearing is a serious problem with ATSR's night-time SST retrieval after the loss of the 3.7μm channel. Jones *et al.* (1996) have proposed a scheme whereby cloud-contaminated night-time observations can be identified by comparison with day-time data, which they assume are not affected by cloud contamination. A dataset which has been subjected to this post-processing scheme is likely to be made available in late 1996, and an improved cloud-clearing algorithm has been developed and is currently being implemented in the operational scheme.

ATSR day-time data are not considered to be seriously affected by cloud contamination. However ATSR's day-time SSTs exhibit a larger cold bias with respect to NOAA-OA SSTs than can be attributed to the skin/bulk effect, and the patterns of water vapour and aerosol contamination are clearly evident. This suggests that the coefficients used in the two-channel retrievals may not be optimal. As mentioned above, the initial nine months of SSTs from the three-channel, night-time observations show no evidence of atmospheric bias. These data may be used directly to provide a "ground truth" in the derivation of unbiased coefficients for a revised two-channel night-time retrieval for use after the 3.7μm channel loss. In conjunction with a model of the diurnal cycle in skin SST, we also intend to use the period when 3.7μm data were available to examine the origins (and scope for removal) of the observed bias in the two-channel day-time retrieval algorithm.

In the longer term, several results presented here, particularly the seasonal cycle in the bias in the two-channel retrieval algorithms, point to the need for a more physically based approach to SST retrieval to exploit the full potential of the ATSR data. Information about total column and vertical profiles of atmospheric moisture and aerosol, while apparently unnecessary for accurate three-channel, dual-view SST retrieval, may significantly improve two-channel SSTs.

ATSR-2, the second instrument in the ATSR series, was launched on board ESA's ERS-2 in April 1995. Global SSTs from this instrument will be available in late 1996 and the improved processing scheme developed for ATSR-2 data will eventually be used to reprocess ATSR-1 observations, with the resulting SSTs given at 10 arcminute resolution. SSTs from the period May–December 1995 will soon be available from both ATSR-1 and ATSR-2. The comparison of these datasets will help to establish the accuracy of both instruments.

Acknowledgments

We would like to thank Albin Závody and John Delderfield for helpful comments and suggestions.

References

Allen M.R. *et al.*, "Global change detection", *Nature*, **370**, 24–25, 1994.

Baran A.J. and Foot J.S., "New application of the operational sounder HIRS in determining a a climatology of sulphuric acid aerosol from the Pinatubo eruption", *J. Geophys. Res.*, **99**, (D12), 25,673–25,679, 1994.

Bailey P., *SADIST Products (Version 500)*, Space Science Department, Rutherford Appleton Laboratory, 1993.

Bailey P., *SADIST-2, v100 products*, (ER-TN-RAL-AT-2164), Space Science Dept., Rutherford Appleton Laboratory, 1995.

Barton I.J. *et al.*, "Validation of the ATSR in Australian Waters", *J. Atmos. Oceanic Technol.*, **12**, 290-300, 1995.

Bottomley M. *et al.*, "Global Ocean Surface Temperature Atlas, Joint Project, United Kingdom Meteorological Office and Massachusetts Institute of Technology", *Her Majesty's Stationary Office, London*, 20pp, 313 plates, 1990.

Delderfield J. *et al.*, "The Along-Track Scanning Radiometer (ATSR) for ERS-1", *Instrumentation for optical remote sensing from space*, Proc. SPIE 589,114, 1986.

Donlon C.J. and Robinson I.S. "Observations of the oceanic thermal skin in the Atlantic ocean, *J. Geophys. Res.*, 1996

Edwards T. *et al.*, "The Along Track Scanning Radiometer – Measurement of Sea-Surface Temperature from ERS-1", *J. British Interplan. Soc.*, **43**, 160–180, 1990.

Forrester T.N. and Challenor P.G., "Validation of ATSR sea-surface temperatures in the Faeroes region", *Int. J. Remote Sens.*, **16**, 15, 2741–2753, 1995.

Harries J.E. *et al.*, "Observations of sea-surface temperature for climate research", *Phil. Trans. Royal Soc. London*, **309**, 381–395, 1983.

Harrison D.L. and Jones C.P., "A user appraisal of ATSR near-real-time products", *Proc. First ERS-1 Symposium*, ESA SP-359, 791–795, 1994.

Jones M.S. *et al.*, "Reducing Cloud Contamination in ATSR Averaged SST data", *J. Atmos. Oceanic Technol.*, **13**, 492–506, 1996.

Minnett P.J., "Consequences of sea-surface temperature variability on the validation and applications of satellite measurements", *J. Geophys. Res.*, **96**, 18,475–18,489, 1991.

Murray, J., "Sea-Surface Temperatures from ATSR (August 1991 - July 1995)" (RAL publication).

Mutlow C.T., *et al.*, "Sea-surface temperature measurements by the along-track scanning radiometer on the ERS-1 satellite: Early results", *J. Geophys. Res.*, **99**, 575–588, 1994.

McClain E.P., *et al.*, "Comparative performance of

AVHRR based multichannel SSTs", *J. Geophys. Res.*, **90**, 11587–11601, 1985.

Reynolds R.W., "A Real-Time global sea-surface temperature analysis", *J. Climate*, **1**, 75–86, 1988.

Reynolds R.W. , "Impact of Mount Pinatubo aerosols on satellite-derived sea-surface temperatures", *J. Climate*, **6**, 768-774, 1993.

Reynolds R.W. and Smith T.M., "Improved global sea-surface temperature analyses using optimum interpolation", *J. Climate*, **7**, 929–948, 1994.

Reynolds R.W. and Marisco D.C., " An Improved Real-Time global sea-surface temperature analysis," *J. Climate*, **6**, 114–119, 1993.

Saunders R.W. and Kriebel K. T., "An improved method for detecting clear sky and cloudy sky radiances from AVHRR data", *Int. J. Remote Sens.*, **9**, 123–150, 1988.

Schluessel P. *et al.*, "On the Bulk-Skin Temperature Difference and Its Impact on Satellite Remote Sensing of Sea-Surface Temperature", *J. Geophys. Res.*, **95**, No. C8, 13341–13356, 1990.

Závody A.M. *et al.*, "The ATSR data processing Scheme Developed for the EODC", *Int. J. Remote Sens.*, **15**, 827–843, 1994.

Závody A.M. *et al.*, "A radiative transfer model for SST retrieval for the ATSR", *J. Geophys. Res.*, **100**, 937–952, 1995.

6 Figures

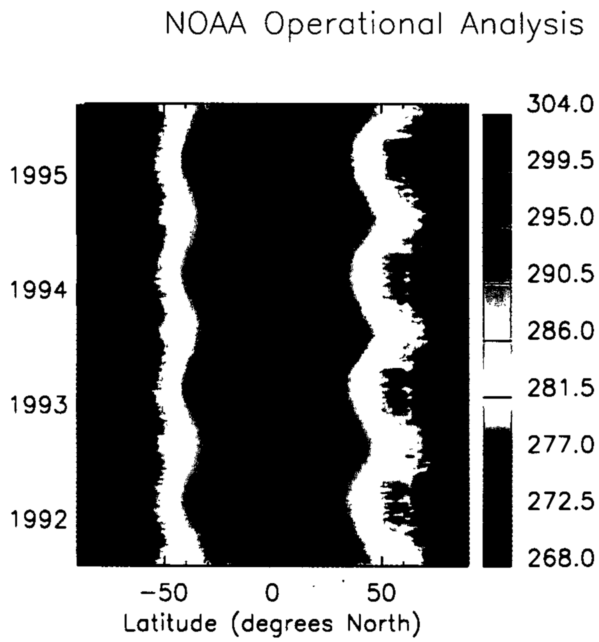

Figure 1. Time-latitude plot of zonal mean SST from the NOAA operational analysis

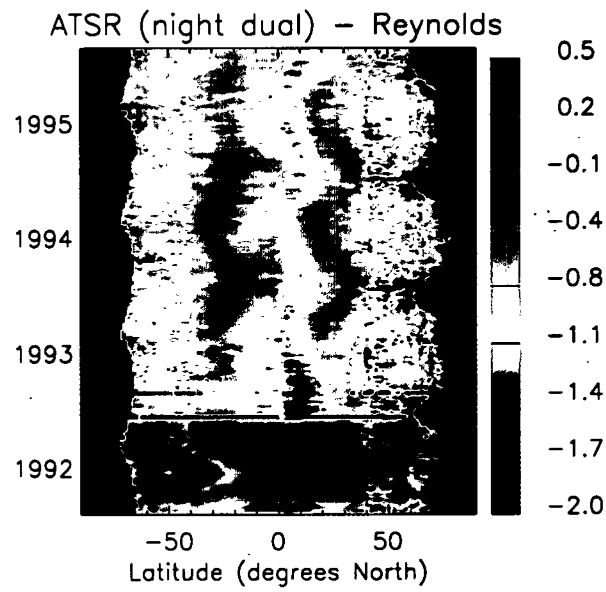

Figure 3. Zonal mean differences between ATSR dual-view night-time SSTs and NOAA-OA. Note revised colour scale

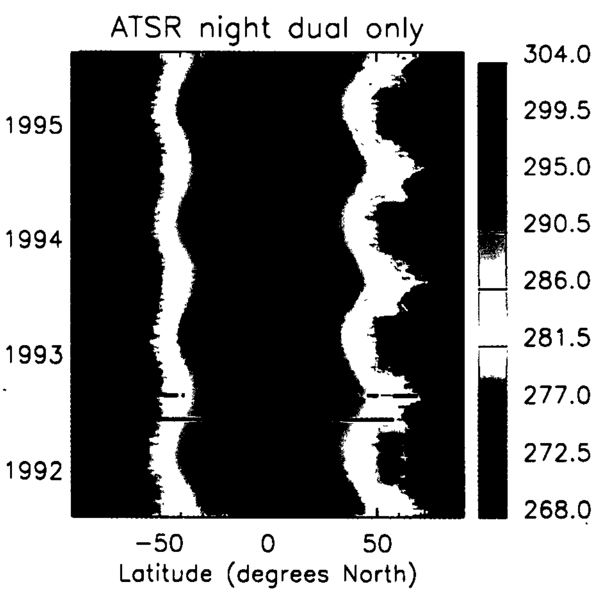

Figure 2. As figure 1, with ATSR dual-view night-time SSTs

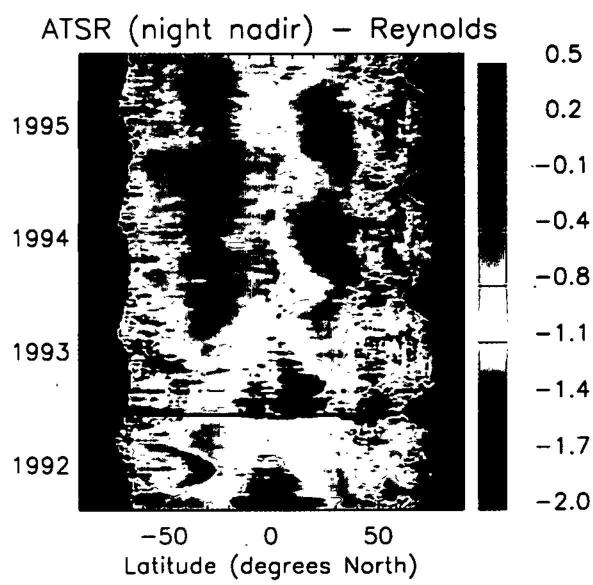

Figure 4. As figure 3, but with ATSR single-view (nadir only) night-time SSTs

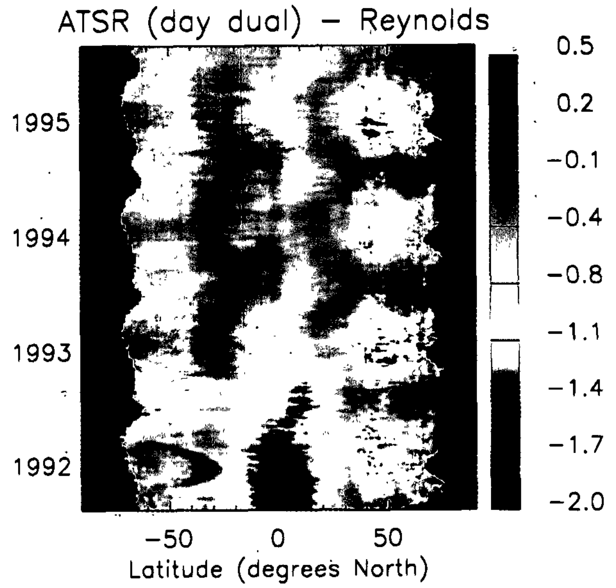

Figure 5. Zonal mean differences between ATSR dual-view day-time SSTs and NOAA-OA.

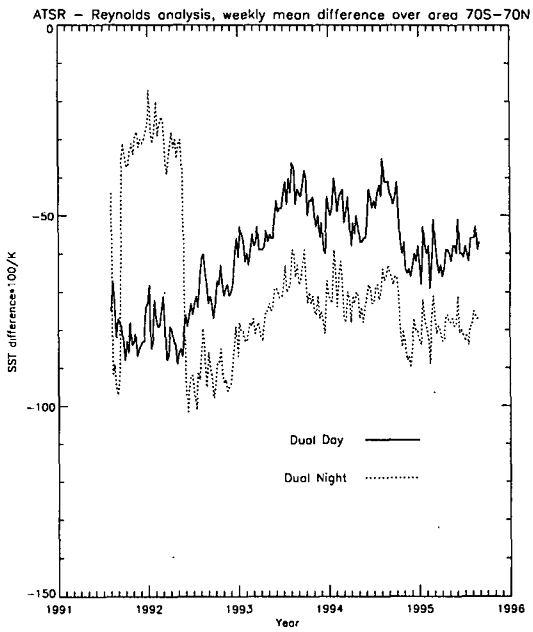

Figure 7. Area mean difference between ATSR dual-view SSTs and NOAA-OA in the latitude range 70°S–70°N

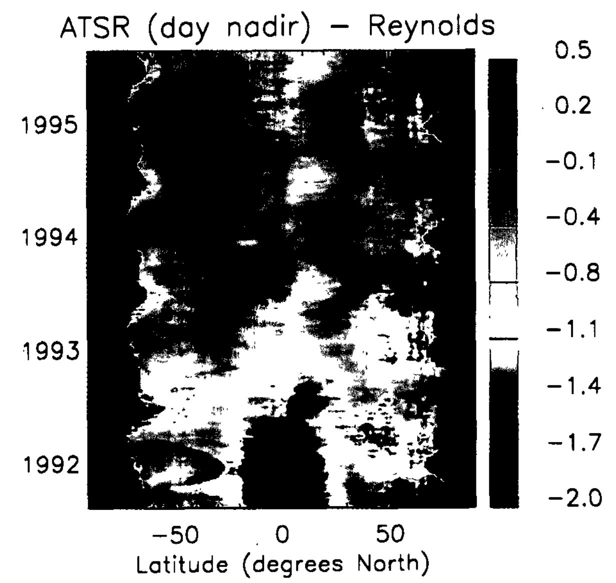

Figure 6. As figure 5, but with ATSR single-view (nadir only) day-time SSTs

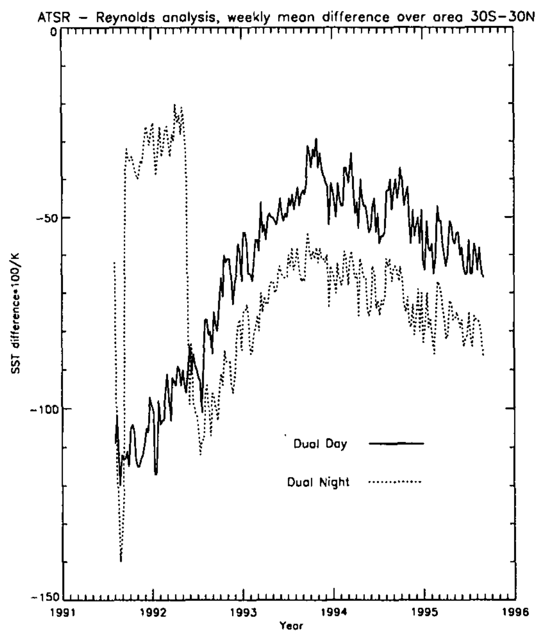

Figure 8. As figure 7, using dual-view data in the latitude range 30°S–30°N

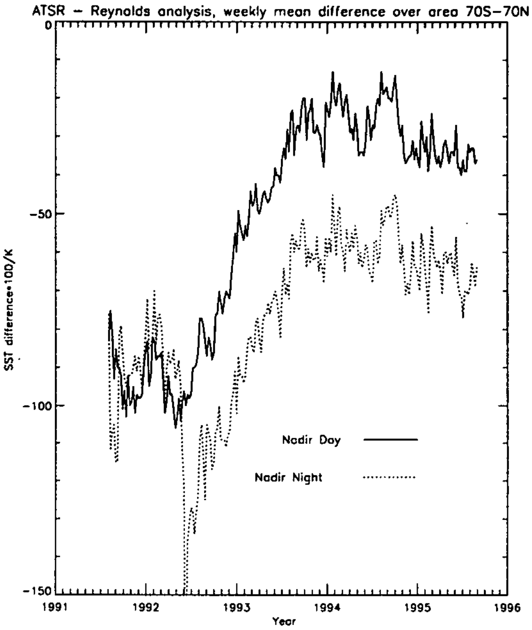

Figure 9. As figure 7, using ATSR single-view (nadir only) SSTs

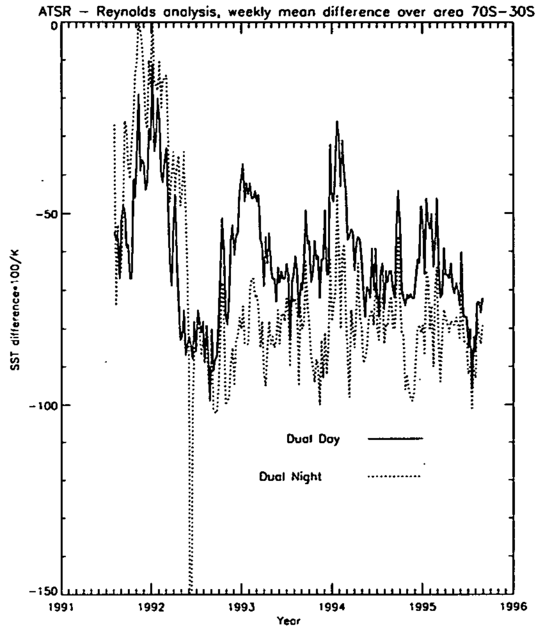

Figure 11. As figure 7, using dual-view data in the latitude range 70°S–30°S

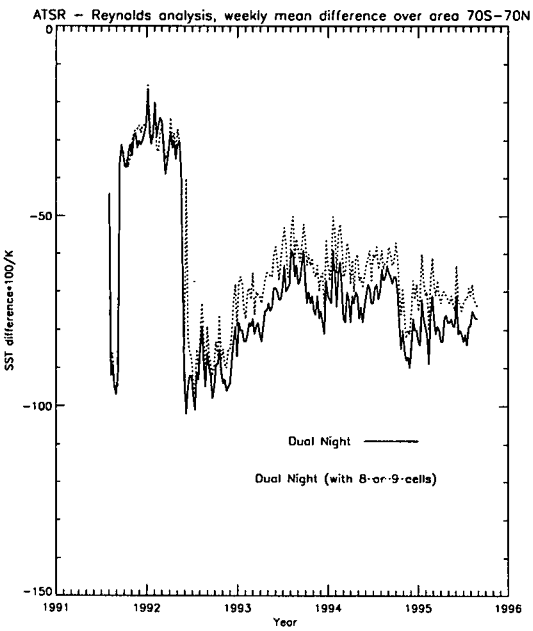

Figure 10. As figure 7, comparing area mean difference averaged over all dual-view SSTs and over only those in which 8 or 9 cells contributed to the ASST value (considered cloud free)

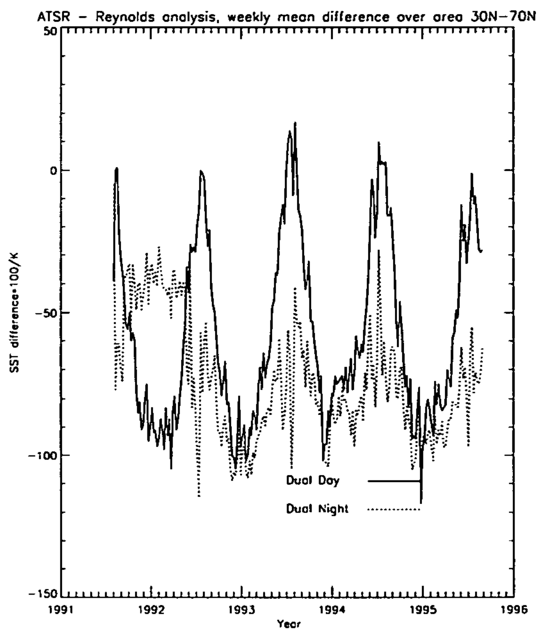

Figure 12. As figure 7, using dual-view data in the latitude range 30°N–70°N

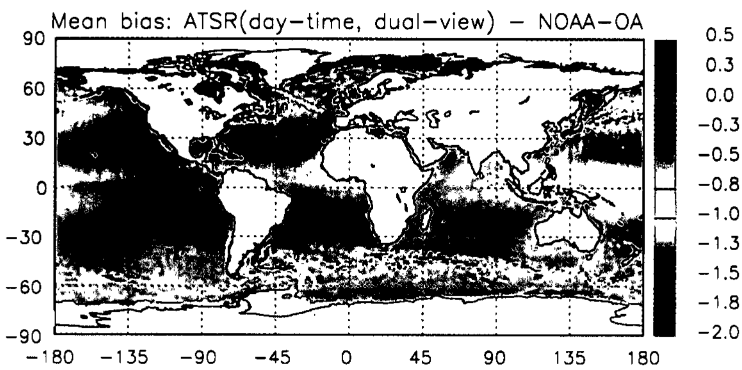

Figure 13. Four-year mean ATSR minus NOAA-OA: ATSR day-time dual-view SSTs only

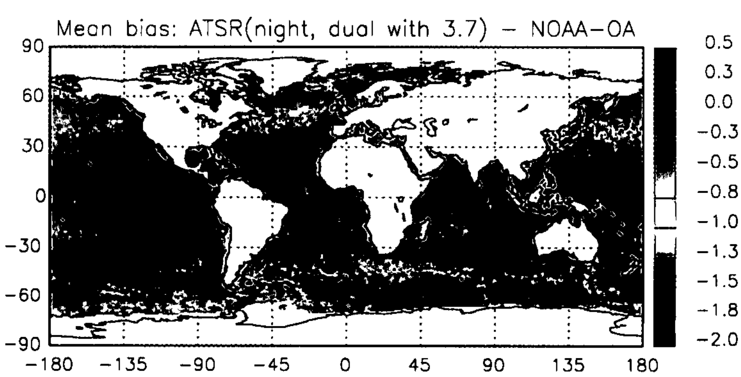

Figure 14. 8-month mean ATSR minus NOAA-OA: ATSR night-time dual-view SSTs for the period (October 1991 to May 1992) with 3.7μm channel data

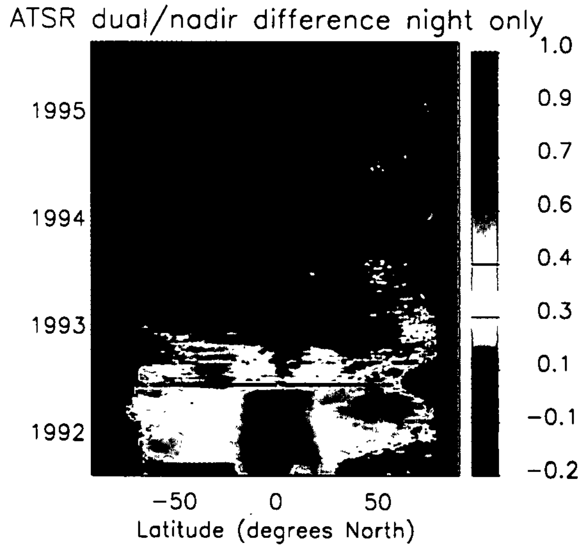

Figure 15. Time-latitude plot of zonal mean difference between ATSR dual-view and ATSR single-view (nadir only) SSTs: night-time data

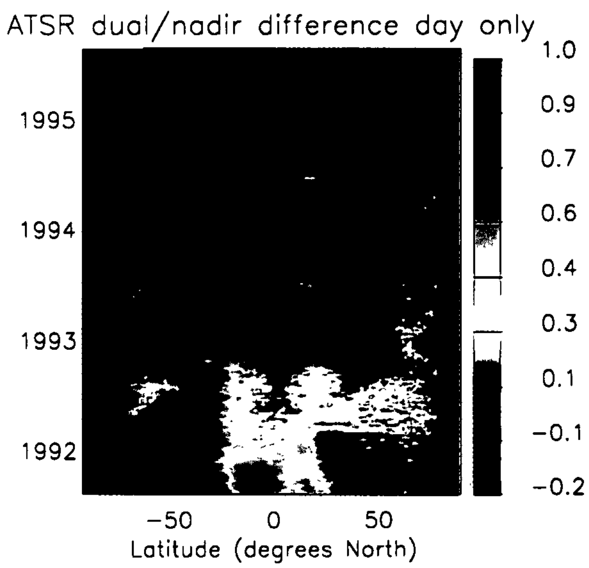

Figure 16. Time-latitude plot of zonal mean difference between ATSR dual-view and ATSR single-view (nadir only) SSTs: day-time-data